Hindawi
Geofluids
Volume 2021, Article ID 7089832, 10 pages
https://doi.org/10.1155/2021/7089832

Research Article

Flow Mechanism and Strength Characteristics of Textile Reinforced Concrete Mixed with Colloidal Nano-SiO_2

Ping Xu,[1] **Rui Shi**,[1] **Chao Wang**,[2] **Yuhao Cui**,[1] **and Minxia Zhang**[1]

[1]*School of Civil Engineering, Henan Polytechnic University, Jiaozuo, 454000 Henan, China*
[2]*China Construction Second Engineering Bureau Ltd., East China Company, Shanghai 200120, China*

Correspondence should be addressed to Chao Wang; ecc_cwang@163.com

Received 19 April 2021; Accepted 31 July 2021; Published 11 August 2021

Academic Editor: Yi Xue

Copyright © 2021 Ping Xu et al. This is an open access article distributed under the Creative Commons Attribution License, which permits unrestricted use, distribution, and reproduction in any medium, provided the original work is properly cited.

In order to develop textile reinforced concrete (TRC) with good flowability and strength, colloidal nano-SiO_2 (CNS) is adopted to improve the performance of TRC. The flowability, compressive strength, flexural strength, and four-point bending tests of TRC matrix with CNS are carried out, and the changes of internal micromorphological characteristics of TRC matrix are analyzed by combining with scanning electron microscopy. The results show that the CNS has an inhibitory effect on the flowability of TRC matrix, and the greater the amount of admixture is, the smaller the slump expansion of TRC matrix is. The compressive strength and flexural strength of TRC matrix show a trend of increasing and then decreasing as the amount of CNS increases, and the compressive strength reaches the maximum at each age (7 d, 14 d, 28 d) when CNS and silica fume replace 5% cement by 1 : 4 equal mass. The flexural strength reaches the maximum at each age (7 d, 14 d, 28 d) when 5% cement is replaced by CNS and silica fume with 3 : 7 equal mass. The flexural strength increases with the increase of CNS admixture. It is found by electron microscope scanning that the incorporation of CNS consumes more $Ca(OH)_2$, refines the $Ca(OH)_2$ crystal size, and generates more C-S-H gels. These C-S-H gels are distributed in a net-like pattern inside the concrete, filling the internal pores, effectively densifying the interfacial transition zone between the cementitious material and the aggregates, and optimizing the internal structure.

1. Introduction

Textile reinforced concrete (TRC) has the superior characteristics of crack resistance, impact resistance, and durability properties, which has been widely applied in lightweight thin-walled structures, such as large span arches, shells, and domes [1–3]. TRC matrix has a better flowability because of the coarse aggregates completely replaced by the fine aggregates with different gradations, but the strength, stiffness, and elastic modulus of TRC matrix are adversely affected [4, 5]. Therefore, developing a fine-grained matrix concrete with good strength and flowability is the first step is to achieve the excellent performance of TRC. In recent years, nanotechnology has made effective progress in improving the mechanical and work-ability properties of cement composites [6].

More studies have shown that incorporation of CNS results in significant increase in compressive and flexural strength of concrete [7, 8]. Hani [9] compared the change in compressive strength of self-compacting concrete at different water-cement ratios after incorporation of appropriate amount of nano-SiO_2 and found higher compressive strength at larger water-cement ratio. Adak et al. [10] studied the effect of nano-SiO_2 on the strength and durability of fly ash based geopolymer mortar and found that the compressive and flexural strength of the oligomeric mortar with 6% nano-SiO_2 added was significantly improved after 28 days. Gülşan [11] found that the combined use of silica nanoparticles and steel fibers greatly increased the compressive strength and flexural properties of the material. Madadi [12] also found that the effect of silica nanoparticles on improving the bond strength of reinforced concrete was greater compared to that of fibers. In addition, incorporation of silica nanoparticles improved the durability of concrete [13]. A study by Li [14] showed that the combined addition of silica fume and nano-SiO_2 further improved the corrosion resistance of sulfate and chloride ions. Nano-SiO_2 also

improved the high temperature resistance of concrete. Wang [15] studied the mechanical properties and microstructure at 25°C, 200°C, 400°C, and 600°C by static load test, scanning electron microscopy, and X-ray diffraction and found that the addition of nano-SiO_2 improved the high temperature performance of concrete at different temperatures. There are two reasons why the mechanical properties of concrete are enhanced by the addition of nano-SiO_2, either because the addition of silica nanoparticles improves the early hydration reaction of concrete [16–18] or because the nanoparticles act as fillers to fill the interfacial transition zone between aggregates and improve the denseness of concrete [19–21]. In summary, it can be tentatively judged that it is a viable option to introduce nano-SiO_2 into the preparation of TRC for improving the mechanical properties of TRC [22, 23]. Therefore, it is the focus of this study to investigate the mechanism of the effect of nano-SiO_2 on the mechanical properties of TRC matrix.

However, a number of studies have shown that the incorporation of nano-SiO_2 affects the flowability of concrete. Yu [24] investigated the effect of nano-SiO_2 on the hydration and microdevelopment of ultra-high performance concrete and found that the viscosity of ultra-high performance concrete increased with the addition of nano-SiO_2. This resulted in more air retention in the mixture and increased porosity of the concrete. Mosavinezha [25] found that the addition of water reducer and air inducing agent (AEA) at 2% and 0.2% by weight of cement, respectively, improved the poor matrix fluidity caused by the addition of nano-SiO_2. Puetens [26] investigated the effect of nano-SiO_2 and carbon nanotubes on self-compacting concrete and found that nano-SiO_2 inhibited concrete segregation, increased water demand, and reduced flowability, but the addition of fly ash reduced the loss of flowability properties. Therefore, it is important to study the mechanism of the effect of nano-SiO_2 on the fluidity of TRC matrix and analyze its microscopic mechanism in order to make the aggregates of TRC can have good workability in the preparation process.

In this paper, a high-performance TRC matrix is formulated by using CNS instead of silica fume to compare the difference in performance between the CNS and silica fume-doped TRC matrix. The changes in the microstructure of the TRC matrix are analyzed to compare the differences between them in improving the interfacial properties and to reveal the mechanism of the effect of CNS on the performance of fine-grained concrete. These experiments in this paper are designed to further investigate the effect of nano-SiO_2 on the flowability and strength of TRC matrix.

2. Test Materials and Test Design

2.1. Materials

2.1.1. Cementitious materials. The cementitious material consists of cement, fly ash, and silica fume. The P. O 42.5 cement has a specific surface area of 362 m^2/kg and apparent density of 3.11 g/m^3. The specific surface area of silica fume (SF) is 30000 m^2/kg and apparent density of 2.23 g/m^3. The cementitious material chemical composition is shown in Table 1.

Table 1: Chemical compositions of cementitious materials (w_t/%).

Materials	SiO_2	CaO	Al_2O_3	Fe_2O_3	MgO	Loss
Cement	22.85	60.16	6.18	3.85	2.15	4.81
Fly ash	49.91	3.72	37.69	4.40	0.55	3.73
Silica fume	93.52	0.32	0.31	0.73	0.12	3.81

2.1.2. Colloidal Nano-SiO_2 (CNS). The nano-SiO_2 is made of colloidal nano-SiO_2 (CNS) with an average particle size of 13 nm, a solid content of 30%, and a sample purity of more than 99%. The physical properties are shown in Table 2.

2.1.3. Sand. Two types of river sand with particle sizes of 0 ~ 0.6 mm and 0.6 ~1.2 mm are used for the experiments, to ensure good working performance of fine-grained concrete.

2.1.4. Water reducer. Polycarboxylic acid high efficiency water reducer with water reduction rate > 30% is used to preparate the TRC matrix.

2.2. Mix Properties. In this test, silica fume is mixed with CNS for the TRC matrix with a water-cement ratio of 0.38, a cement-sand ratio of 0.7.20% cement is replaced by equal mass of fly ash in the cementitious material, and 5% cement is replaced by equal mass of silica fume and CNS in different proportions. The amount of CNS is 0.5%, 1%, 1.5%, and 2%, respectively, according to the solid content of nano-SiO_2 as a percentage of the mass of cementitious material. The amount of water reducer is 0.7% of the total mass of cementitious material. The mix properties of TRC matrix are shown in Table 3.

2.3. Test Method

2.3.1. Specimen Preparation. The TRC matrix is mixed by a forced mixer. Firstly, sands of two different grain sizes are mixed for 2 minutes; then, cement, fly ash, and silica fume are added to the mixer for 5 minutes dry to mix the sand with the cementitious material. Then, the water reducer is added to the mixer with 1/4 of water and mixed at slow speed for 2 minutes, pouring the CNS and the remaining water into the mixture, mixing quickly for 1 minute, and finally loading to the standard triplex test mold with the specification of 40 mm × 40 mm × 160 mm for molding. When the CNS is mixed with more, it is properly vibrated according to the test condition. The molded specimens are placed in the standard curing room for 24 h and then demolded. The demolded specimens are placed in the standard curing room (temperature (20 ± 2°C), relative humidity 95% or more) and cured to different ages and then tested for compressive and flexural strength.

2.3.2. Slump Expansion. In this paper, the slump expansion test is used to evaluate the fluidity of TRC matrix after CNS modification according to GB/T 2419-2005 [27]. For the slump expansion test, a slump cylinder with an upper opening diameter of 100 mm, a lower opening diameter of 200 mm, and a height of 300 mm is used. Firstly, the aggregate mix was poured into the slump cylinder, and each time

Table 2: Physical properties of CNS.

Product model	Appearance	SiO_2 content	pH	Density	Viscosity	Particle size
GS-30	Lightly milky	30.5%	9.6	1.204 g/cm^3	6.2 cP	13 nm

Table 3: Mix properties of TRC matrix (kg/m^3).

Number	Cement	Fly ash	Silica fume	CNS	Sand (mm)		Water	Water reducer	Flowability (cm)
					0 ~ 0.6	0.6 ~1.2			
A	472	168	35	—	325	650			82
S1	472	168	31.6	11.3	325	650			76
S2	472	168	28.2	22.5	325	650	256.5	6.1	69
S3	472	168	25	33.8	325	650			38
S4	472	168	21.5	45	325	650			33

Note: No. A is the reference group; S1 to S4 are the CNS modified groups.

the amount poured was 1/3 of the volume of the slump cylinder. Then, the slump cylinder was lifted vertically and smoothly so that the concrete could flow freely, when the concrete is no longer flowing, measure the diameter of the two extensions in the mutual vertical direction and as shown in Figure 1. In order to meet the self-compaction requirement of the TRC matrix, the flow expansion is not less than 550 mm.

2.3.3. Compressive Strength and Flexural Strength. The test is carried out according to GB/T 17671-1999 to study the effect of different dosings of CNS on the compressive strength and flexural strength of fine-grained concrete [28]. The flexural strength is tested by using 40 mm × 40 mm × 160 mm prismatic specimens, three specimens are formed for each ratio, and the loading speed is constant at 50 N/s. After the flexural strength test, the fractured specimens are taken for the compressive strength test, and the loading speed is 2.4 kN/s for each group of three specimens.

2.3.4. Four-Point Bending Test. The flexural strength of the TRC is tested by the four-point bending test, which consists of a woven fiber mesh and a matrix doped with nano-SiO_2, with the dimensions of 280 mm × 50 mm × 12 mm. The mold is demolded after 24 h of curing at room temperature, then standard curing is carried out, and the formed sheet is loaded by the four-point bending test. The schematic diagram of the formed sheet and the four-point bending test are shown in Figure 2.

2.3.5. Microscopic Tests. After the specimen is maintained to 60 days for compressive testing, a small number of fragments are removed as samples for testing. The small pieces are impregnated in anhydrous ethanol to terminate hydration before the sample test and dried in a vacuum drying oven at 60°C for half a day, and after drying, the sample surface is gold plated with 20 nm for conductivity by vacuum sputtering [29]. The test acceleration voltage is 10-15 kV, and the acceleration current is adjusted according to the image quality.

Figure 1: Test of slump flow.

3. Discussion and Analysis of Test Results

3.1. Effect of CNS on the Flowability of TRC Matrix. The variation of slump expansion of fine-grained concrete at 0, 0.5%, 1.0%, 1.5%, and 2% of CNS admixture is shown in Figure 3. The slump expansion of TRC matrix decreases in different magnitudes with the increase of CNS admixture. The slump expansion of TRC matrix decreases by 59.8% compared with the TRC matrix without CNS, when the amount of CNS is 2%. When the amount of CNS is increased from 0.5% to 1.5%, the slump expansion of fine-grained concrete is reduced by 25.6%, 32.9%, and 53.7% relative to that of unadulterated CNS. The incorporation of water reducer thins the thickness of the surface water and improves the fluidity by repulsion between cement particles, but the amount of filled water does not change. The average particle size of silica particles in CNS is 13 nm, which fills the cement particle gap and improves the compactness, reducing the amount of filling water on the one hand, but increasing the specific surface area on the other hand. Therefore, in the case of the constant water-cement ratio, the effect of CNS on the slump flow of fine-grained concrete depends on the contrast between its filling effect and surface water absorption effect.

The addition of CNS affects the fluidity of concrete for two main reasons. On the one hand, because CNS has a large specific surface area, with the increase of CNS admixture, the

(a) Preparation of specimens (b) Four-point bending test

Figure 2: Textile reinforced concrete and four-point bending test.

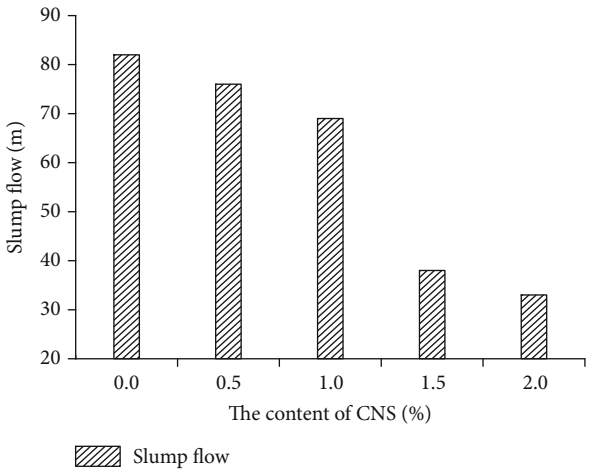

Figure 3: Slump flow expansion of TRC matrix.

required surface water increases rapidly, which increases the water requirement of concrete. On the other hand, CNS further refines the fineness of the cementitious material, which has strong water absorption and is easy to produce flocculation during the mixing process, wrapping the surrounding water in it. Under the combined effect of the above factors, the free water around the cement particles is reduced, thus decreasing the fluidity of the TRC matrix. The slump expansion of fine-grained concrete decreases slowly, when the amount of CNS is between 0 and 1%; when the amount of CNS is greater than 1%, the slump expansion of fine-grained concrete is less than 550 mm and no longer meets the liquidity requirements.

3.2. Effect of CNS on the Compressive Strength of TRC Matrix. The changes of postfolding compressive strength of fine-grained concrete at different ages (7 d, 14 d, 28 d) with the increase of CNS admixture are shown in Figure 4. The postfolding compressive strength of fine-grained concrete at each age increases from 0 to 1.5%. Compared with the compressive strength of the reference group (mixed with 5% silica fume), the compressive strength of each modified group increases by 17.4%, 23.9%, and 8.8% at the age of 7 days, shown in Figure 4(a). The compressive strength of each modified group increases by 16.6%, 28.9%, and 16.6% at the age of 14 days, shown in Figure 4(b). The compressive strength of each modified group increases by 4.6%, 14.9%, and 1.8% at the age of 28 days, shown in Figure 4(c). The compressive strength of each modified group at the age of 60 days increases by 9.4%, 19.9%, and 12.7%, respectively, shown in Figure 4. The compressive strength of fine-grained concrete at each age shows a decreasing trend as the amount of CNS admixture continues to increase to 2%. When the appropriate amount of CNS is incorporated into the fine-grained concrete (less than 1.5%), due to the extremely small particle size of CNS (average particle size of 13 nm), it increases the matrix compactness by refining the internal pores of fine-grained concrete and finally improves the compressive strength of the specimens.

On the one hand, the incorporation of CNS forms monomers of silicon (e.g., $-OSi(OH)_3$, $-OSi(OH)_2$) in the fine-grained concrete, and these monomers combine with $Ca(OH)_2$ generated by the reaction of cement to form C-S-H gels filled into the microscopic pores of fine-grained concrete, thus defensing the microstructure of the matrix and improving the compressive strength of the specimens. On the other hand, the test uses a large proportion of SiO_2 and Al_2O_3 in the fly ash, the fly ash activity is low, and the ratio of $n(SiO_2)/n(Al_2O_3)$ in the slurry has a greater degree of influence on its compressive strength. With the increase of CNS admixture, the concentration of silicon monomer in the matrix gradually increases, promoting the secondary hydration reaction of fly ash and the formation of three-dimensional mesh structure of silica-aluminate gel. When the amount of CNS is greater than the optimal value of 1%, the system of excessive SiO_2 is easy to deposit on the surface of the cement particles, combined with H_2O reaction, reducing the water required for cement hydration, unfavorable to the polymerization reaction, and reducing the compressive strength of fine-grained concrete gradually.

3.3. Effect of CNS on the Flexural Strength of TRC Matrix. The variation law of flexural strength of fine-grained concrete at different ages (7 d, 14 d, 28 d) with the increase of CNS admixture is shown in Figure 5. The postfolding compressive strength of fine-grained concrete at all ages increases in different magnitudes, when the amount of CNS is increased

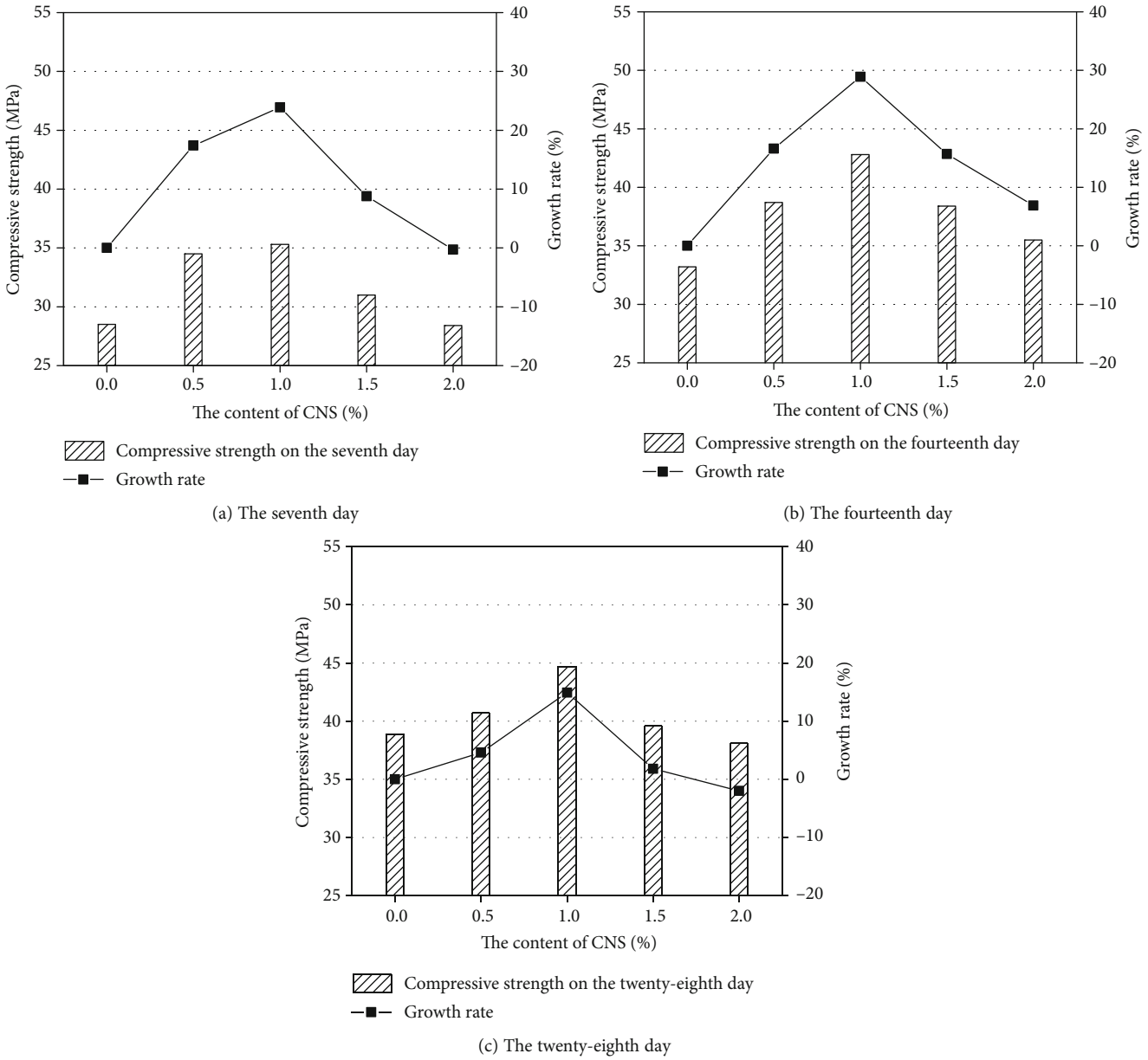

Figure 4: Effect of CNS dosing on compressive strength at different ages.

from 0 to 2%. Compared with the base group (with 5% silica fume), the flexural strength of each modified group increases by 0%, 25%, 44.4%, and 14.4% at 7 days of age, shown in Figure 5(a)and 5.9%, 17.6%, 23.5%, and 19.6% at 14 days of age, shown in Figure 5(b). The flexural strength of each modified group increases by 9.5%, 12.7%, 23.8%, and 19.6% at 28 days of age, respectively, shown in Figure 5(c). With the continuous increase of CNS admixture, the growth of flexural strength of fine-grained concrete at each age shows a trend of first increase and then decrease.

When the admixture amount is 1.5%, the flexural strength at all ages reaches the maximum. After adding CNS, the cement particle gaps are filled by nano-SiO_2, which reacts with $Ca(OH)_2$, and the hydration product of cement. Hydrated calcium silicate gel is distributed between cement particles in a net shape and connected cement particles together. In the process of concrete tension, it weakens the pore stress concentration and increases the tensile stress of the matrix. Since the denser the internal structure of concrete is, the higher the energy required to be absorbed during crack expansion is, and the increase of flexural strength is facilitated.

3.4. Effect of CNS on the Bending Capacity of TRC. The bending cracking stress and ultimate stress of TRC with different doping of CNS are shown in Figure 6, and the bending cracking stress and bending ultimate stress of the specimens are significantly increased with the increase of CNS doping. The flexural cracking stresses of TRC with 0.5, 1, 1.5, and 2 CNS doping increase by 2.3%, 8.6%, 34.1%, and 95.5%, respectively, and the flexural ultimate stresses increase by 49.4%, 56.8%, 51.4%, and 72.7%, respectively, compared with

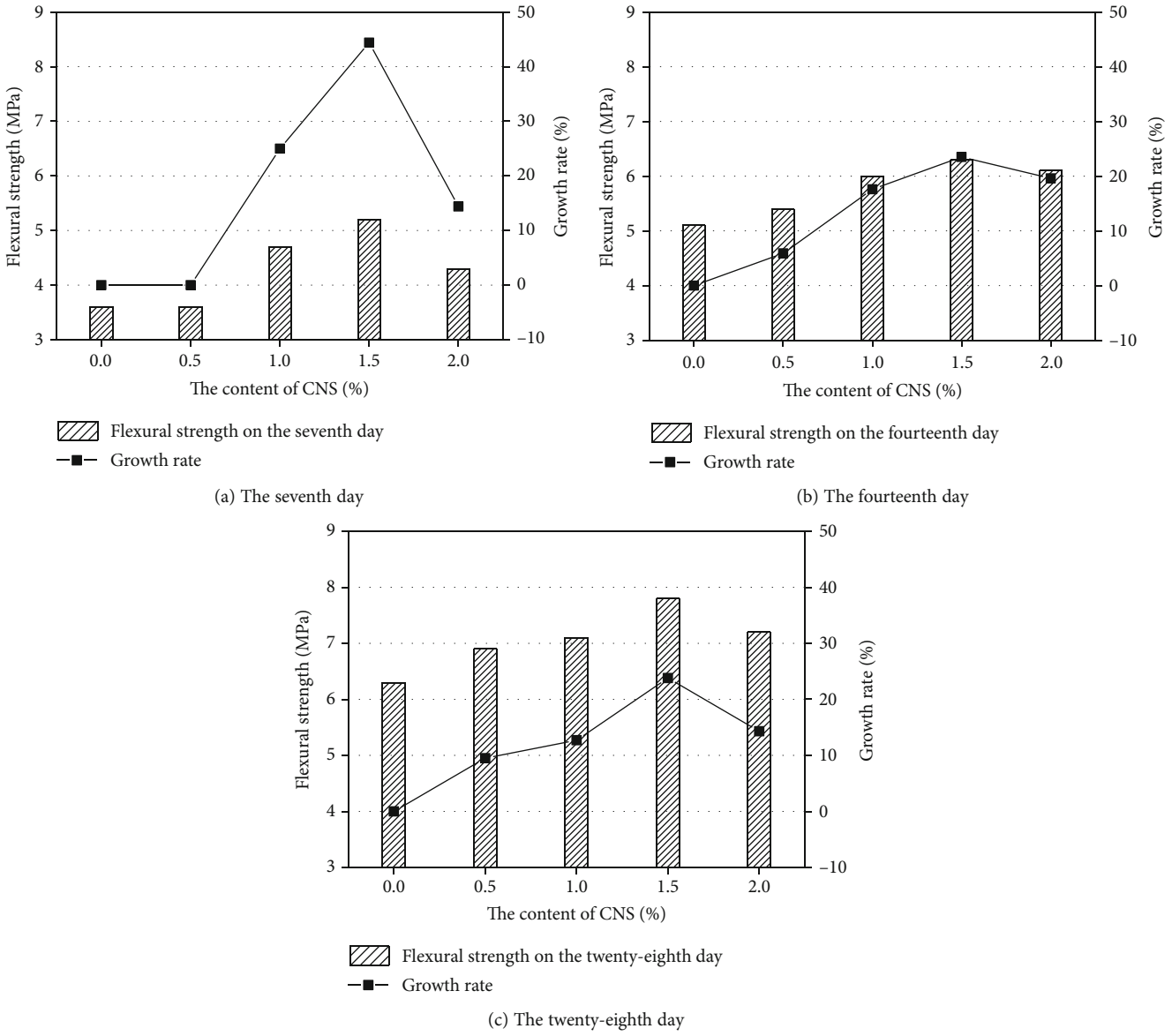

Figure 5: Effect of CNS doping on flexural strength at different ages.

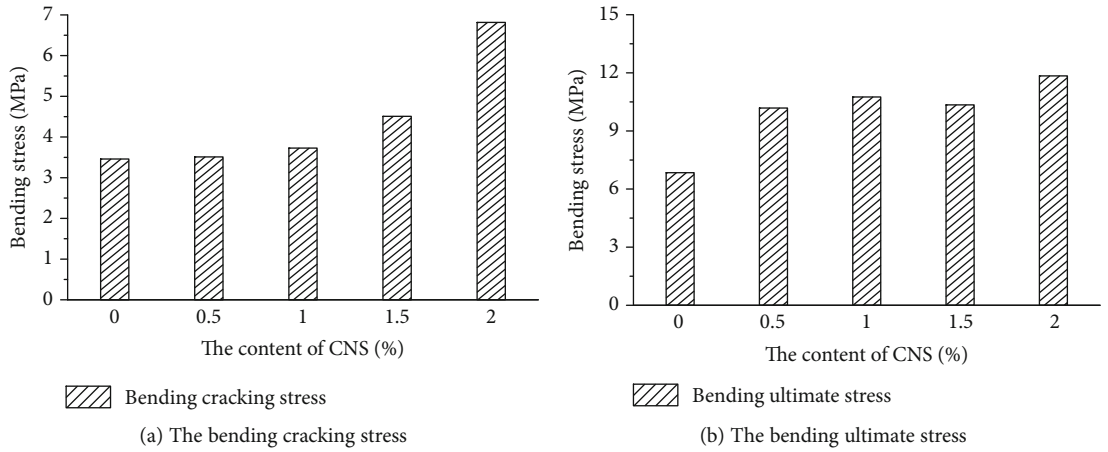

Figure 6: Bending cracking stress and ultimate stress of TRC with different doping of CNS.

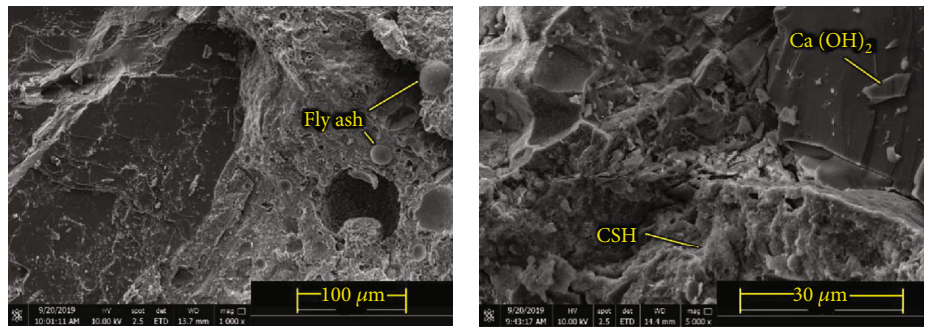

(a) Fly ash (b) Hydration products

Figure 7: Microscopy images of fine grained concrete.

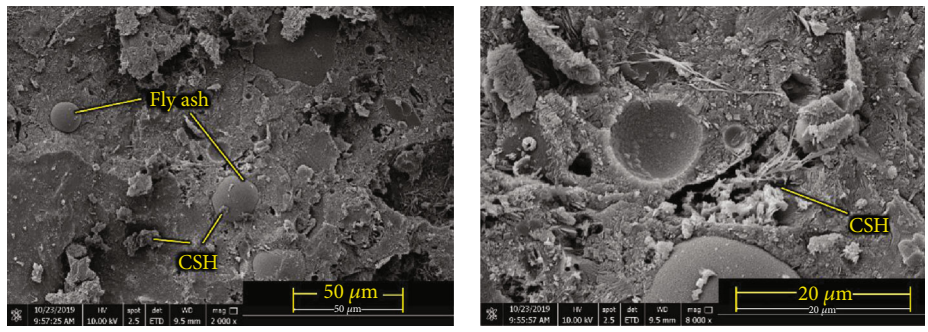

(a) Hydration products on the surface of fly ash (b) Flocculent C-S-H gel

Figure 8: Microscopy images of designed fine grained concrete with 0.5% CNS.

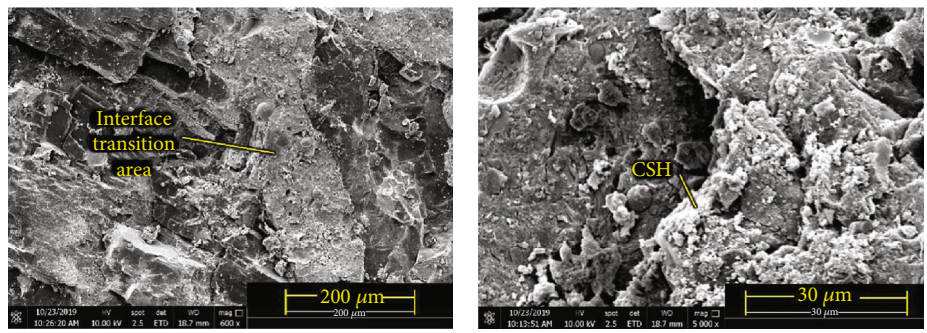

(a) The interface transition area (b) Hydration products

Figure 9: Microscopy images of designed fine grained concrete with 1% CNS.

those of TRC without CNS doping. When basalt fiber fabric is laid out, the load-bearing capacity of TRC sheet is higher than that of the sheet specimens without CNS, and the load-bearing capacity of the sheet increases with the increase of CNS doping in the dosing range of this test. Therefore, the bending test data of each group of specimens show that the higher the doping of CNS is, the more beneficial for improving the flexural load bearing capacity of TRC in the doping range of this test is.

The main reason for the lower strength of the TRC without CNS is that the strength of the fine-grained concrete is lower, the fluidity is poorer, and less fine-grained concrete is invaded inside the fiber bundles. Only the outer fiber roving is bonded to the matrix, and the inner and outer fiber filaments are not synergistically stressed during the stressing process of the thin plate. Therefore, the inner fiber yarn is pulled out sequentially, and bond slip damage occurs, which leads to a decrease in specimen load. However, for the specimens with CNS, the presence of CNS makes the hydration reaction of the TRC matrix more adequate and the bonding with the fibers more tight; therefore, the bending cracking stress of TRC is enhanced by the external nano-SiO_2 doping.

3.5. Microscopic Morphology Analysis. Scanning electron microscopy analysis results demonstrating the internal microstructural morphology of mixed-doped fine-grained concrete and CNS after 28 days of curing are shown in Figures 7–9. A common feature is demonstrated in all of

these micromorphological feature maps. When CNS is employed together with silica fume, the interface between the aggregate particles and the hardened cement matrix is effectively densified, resulting in a denser bond between the aggregate and cement interface and an increase in the hardness of the interface transition zone. In addition to the change in interface transition, other structures in the matrix become dense.

The microscopic morphology of the benchmark group is shown in Figure 7. When it is magnified to 1000 times, the natural fine sand particles are tightly bound to the cement paste interface; in addition, the fly ash are not involved in hydration, silica fume particles form solid glass spheres, and hollow spherical shells exist. The surface of the spheres is smooth, and no hydration products are generated, indicating that the hydration reaction of fly ash and silica fume is incomplete, which plays the role of filler. When is magnified to 5000 times, the honeycomb pores between the interface of the aggregate and the cement paste are obvious. The partially intact $Ca(OH)_2$ crystals are attached to the surface of the aggregate and are arranged in a directional distribution, tending to form a directional layer, which is conducive to the emergence of pores and microcracks.

The changes in the microstructure of the fine-grained concrete with the addition of 0.5% CNS are shown in Figure 8, comparing the benchmark group specimens. At a magnification of ×2000, the hydration products are shown on the surface of the fly ash. The synthesized C-S-H gel is mainly presented as flocs or flakes, wrapped around the fly ash in a laminar distribution, and a small amount of layered $Ca(OH)_2$ crystals is observed as the reaction residue of the synthesized C-S-H gel. When it is magnified to ×8000, the fibrous filamentous hydration products form a continuous whole, filling the microscopic cracks within the concrete. The hydration product crystals grow in empty spaces (e.g., larger capillaries) or in entrapped pores, refining the pores and densifying the concrete structure.

The change in the interfacial transition zone between the fine-grained concrete cement matrix and the aggregate particles is shown in Figure 9, when 1.0% CNS is added. The void space between the cement paste and the aggregate particles is completely filled with hydration products, and it is difficult to observe $Ca(OH)_2$ crystals in the interfacial transition zone. On the one hand, the CNS volcanic ash effect consumes a large number of calcium hydroxide crystals, generating more C-S-H gels, reducing the voids, and compacting the interfacial transition zone and cement paste structure; on the other hand, in the hardening stage of the matrix of cementitious materials containing CNS and silica ash, there is a lack or almost no water-filled space around the concrete, and the aggregate is surrounded by a dense and hard matrix with a dense and homogeneous structure.

In summary, the enhancement of the TRC matrix by CNS incorporation is mainly reflected in the strengthening of the interfacial transition zone. One is that the micronized silica fume plays a filling role on the interfacial transition zone, and more importantly, the SiO_2 in CNS reacts with the $Ca(OH)_2$ to generate a C-S-H gel that is more dense than $Ca(OH)_2$, which reduces the voids in the interfacial transition zone.

4. Conclusion

(1) As the water-to-cement ratio is constant, the effect of CNS on the fluidity of the TRC matrix depends on its filling effect and the surface water absorption effect. As the CNS content increases, the slump expansion of fine-grained concrete decreases slowly, when the CNS content is 0%~1%. Besides, the decreased amplitude becomes larger, and the fluidity is poor, when the content is more than 1%

(2) On the one hand, silicon monolayers are formed in fine-grained concrete after adding CNS. These monolayers form $Ca(OH)_2$ that is formed by cement hydration reaction C-S-H, and the gel is filled into the microscopic pores of fine-grained concrete. On the other hand, fly ash secondary hydration is promoted to improve the compressive strength of fine-grained concrete. With the increase of CNS content, the compressive strength of different ages increases first and then decreases. When the CNS content is 1, the compressive strength of each age is the largest

(3) The filling effect of CNS makes the hydrated calcium silicate gel distribute between cement particles in a network. During the tensile process of concrete, the pore stress concentration is weakened, and the tensile stress of the matrix is increased. Thus, the flexural strength of fine-grained concrete is improved. With the increase of CNS content, the flexural strengths in different ages increase first and then decrease. When the CNS is 1.5, the flexural strength of each age is the largest

(4) A large amount of $Ca(OH)_2$ crystals with directional distribution in the interface transition region are consumed by the use of CNS, which reduce the internal pores, and dense the internal structure, and effectively improve the interfacial properties between aggregate particles and hardened cement matrix, thereby enhancing the strength of fine-grained concrete

Data Availability

The data used to support the findings of this study are included within the article.

Conflicts of Interest

The authors declare that they have no conflicts of interest.

Acknowledgments

The Youth Key Teacher Project of Henan Provincial Colleges and Universities (2017GGJS054), Financial Supports from the Key Science and Technology Program of Henan Province, China (No. 202102310253), Joint Funds of the National Natural Science Foundation of China (No. U1904188), the Doctor Foundation of Henan Polytechnic University (No. B2016-67), and the Science and Technology Project of Henan

Provincial Department of Transportation, China (No. 2019J-2-13) are gratefully appreciated.

References

[1] J. Hegger and S. Voss, "Investigations on the bearing behaviour and application potential of textile reinforced concrete," *Engineering Structures*, vol. 30, no. 7, pp. 2050–2056, 2008.

[2] V. Mechtcherine, "Novel cement-based composites for the strengthening and repair of concrete structures," *Construction and Building Materials*, vol. 41, pp. 365–373, 2013.

[3] R. Contamine, A. S. Larbi, and P. Hamelin, "Contribution to direct tensile testing of textile reinforced concrete (TRC) composites," *Materials Science & Engineering A*, vol. 528, no. 29-30, pp. 8589–8598, 2011.

[4] N. Shafiq, R. Kumar, M. Zahid, and R. Tufail, "Effects of modified metakaolin using nano-silica on the mechanical properties and durability of concrete," *Materials*, vol. 12, no. 14, p. 2291, 2019.

[5] Y. Xue, F. Gao, Y. N. Gao, X. Liang, Z. Z. Zhang, and Y. Xing, "Thermo-hydro-mechanical coupled mathematical model for controlling the pre- mining coal seam gas extraction with slotted boreholes," *International Journal of Mining Science and Technology*, vol. 27, no. 3, pp. 473–479, 2017.

[6] T. Suwan, P. Jitsangiam, and P. Chindaprasirt, "Influence of nano-silica dosage on properties of cement paste incorporating with high calcium fly ash," *Key Engineering Materials*, vol. 4874, pp. 9–13, 2020.

[7] Z. Z. Cao, Y. L. Ren, Q. T. Wang, B. H. Yao, and X. C. Zhang, "Evolution mechanism of water-conducting channel of collapse column in karst mining area of Southwest China," *Geofluids*, vol. 2021, Article ID 6630462, 8 pages, 2021.

[8] Y. Xue, P. G. Ranjith, F. Dang et al., "Analysis of deformation, permeability and energy evolution characteristics of coal mass around borehole after excavation," *Natural Resources Research*, vol. 29, no. 5, pp. 3159–3177, 2020.

[9] N. Hani, O. Nawawy, K. S. Ragab, and M. Kohail, "The effect of different water/binder ratio and nano-silica dosage on the fresh and hardened properties of self-compacting concrete," *Construction and Building Materials*, vol. 165, no. 20, pp. 504–513, 2018.

[10] D. Adak, M. Sarkar, and S. Mandal, "Effect of nano-silica on strength and durability of fly ash based geopolymer mortar," *Construction and Building Materials*, vol. 70, no. 20, pp. 453–459, 2014.

[11] M. E. Gülşan, R. Alzeebaree, A. A. Rasheed, A. Niş, and A. E. Kurtoğlu, "Development of fly ash/slag based self-compacting geopolymer concrete using nano-silica and steel fiber," *Construction and Building Materials*, vol. 211, pp. 271–283, 2019.

[12] A. Madadi, H. Eskandari-Naddaf, and M. N. Nejad, "Evaluation of bond strength of reinforcement in concrete containing fibers, micro-silica and nano-silica," *Journal of Stress Analysis*, vol. 3, no. 1, pp. 11–19, 2018.

[13] T. A. Tawfik, M. A. El-Yamani, and S. A. El-Aleem, "Effect of nano-silica and nano-waste material on durability and corrosion rate of steel reinforcement embedded in high-performance concrete," *Asian Journal of Civil Engineering*, vol. 20, no. 1, pp. 135–147, 2019.

[14] L. G. Li, J. Y. Zheng, and P. L. Ng, "Cementing efficiencies and synergistic roles of silica fume and nano-silica in sulphate and chloride resistance of concrete," *Construction and Building Materials*, vol. 223, pp. 965–975, 2019.

[15] Y. G. Wang, S. P. Li, H. Peter, and Y. H. Fan, "Mechanical properties and microstructure of basalt fibre and nano-silica reinforced recycled concrete after exposure to elevated temperatures," *Construction and Building Materials*, vol. 247, 2020.

[16] C. Gunasekara, M. Sandanayake, Z. Zhou, D. W. Law, and S. Setunge, "Effect of nano-silica addition into high volume fly ash-hydrated lime blended concrete," *Construction and Building Materials*, vol. 253, p. 119205, 2020.

[17] J. Wang, Y. Cheng, L. Yuan et al., "Effect of nano-silica on chemical and volume shrinkage of cement-based composites," *Construction and Building Materials*, vol. 247, p. 118529, 2020.

[18] Y. Xue, J. Liu, F. Dang, X. Liang, S. Wang, and Z. Ma, "Influence of CH_4 adsorption diffusion and CH_4-water two-phase flow on sealing efficiency of caprock in underground energy storage," *Sustainable Energy Technologies and Assessments*, vol. 42, article 100874, 2020.

[19] N. Zabihi and M. Hulusi Ozkul, "The fresh properties of nano silica incorporating polymer-modified cement pastes," *Construction and Building Materials*, vol. 168, no. 7, pp. 570–579, 2018.

[20] W. L. Shen, J. B. Bai, W. F. Li, and X. Y. Wang, "Prediction of relative displacement for entry roof with weak plane under the effect of mining abutment stress," *Tunnelling and Underground Space Technology*, vol. 71, pp. 309–317, 2018.

[21] Y. Yue, Y. Zhou, F. Xing, G. Gong, B. Hu, and M. Guo, "An industrial applicable method to improve the properties of recycled aggregate concrete by incorporating nano-silica and micro- $CaCO_3$," *Journal of Cleaner Production*, vol. 259, article 120920, 2020.

[22] J. Yu, M. Zhang, G. Li, J. Meng, and C. Leung, "Using nano-silica to improve mechanical and fracture properties of fiber- reinforced high-volume fly ash cement mortar," *Construction and Building Materials*, vol. 239, article 117853, 2020.

[23] Y. Xue, T. Teng, F. Dang, Z. Ma, S. Wang, and H. Xue, "Productivity analysis of fractured wells in reservoir of hydrogen and carbon based on dual-porosity medium model," *International Journal of Hydrogen Energy*, vol. 45, no. 39, pp. 20240–20249, 2020.

[24] R. Yu, P. Spiesz, and H. J. H. Brouwers, "Effect of nano-silica on the hydration and microstructure development of Ultra-High Performance Concrete (UHPC) with a low binder amount," *Construction and Building Materials*, vol. 65, no. 9, pp. 140–150, 2014.

[25] S. H. G. Mosavinezhad and G. F. Pasikhani, "Fresh performance and corrosion resistance of self-compacting concrete containing nano-silica," *Journal of Research in Science and Engineering*, vol. 1, no. 11, 2019.

[26] J. Puentes, G. Barluenga, and I. Palomar, "Effects of nano-components on early age cracking of self-compacting concretes," *Construction & Building Materials*, vol. 73, no. 6, pp. 89–96, 2014.

[27] Y. Xue, J. Liu, P. G. Ranjith, X. Liang, and S. Wang, "Investigation of the influence of gas fracturing on fracturing characteristics of coal mass and gas extraction efficiency based on a multi-physical field model," *Journal of Petroleum Science and Engineering*, vol. 206, article 109018, 2021.

[28] Z. Z. Cao, P. Xu, Z. H. Li, M. X. Zhang, Y. Zhao, and W. L. Shen, "Joint bearing mechanism of coal pillar and backfilling body in roadway backfilling mining technology," *CMC-Computers Materials & Continua*, vol. 54, no. 2, pp. 137–159, 2018.

[29] L. Zhu, F. Dang, Y. Xue, K. Jiao, and W. Ding, "Multivariate analysis of effects of microencapsulated phase change materials on mechanical behaviors in light-weight aggregate concrete," *Journal of Building Engineering*, vol. 42, article 102783, 2021.